actuators

MDPI

Article

Retrofitting Battery Electric Machinery with Unchanged Hydraulic System and Enhanced Control Strategies

Marco Ferrari *, Daniele Beltrami and Stefano Uberti

Department of Industrial and Mechanical Engineering, University of Brescia, Via Branze 38, 25123 Brescia, Italy; daniele.beltrami@unibs.it (D.B.); stefano.uberti@unibs.it (S.U.)
* Correspondence: marco.ferrari3@unibs.it

Abstract: The push for environmental sustainability has accelerated the acceptance of electric vehicles, as well as the exploration of electrified Non-Road Mobile Machinery. This study emphasizes the challenges of electrifying off-highway machinery, which include the many machinery layouts and the presence of Small- and Medium-sized Enterprises in the market. Recognizing the barriers faced by these companies, this paper shows how modeling and simulation can be effective tools for system integration and control optimization, even when lacking extensive expertise in the topic. However, it emphasizes the need for user-friendly modeling tools and methods adaptable to the operational needs of Small- and Medium-sized Enterprises. This study presents a case study of a retrofitted battery-electric hydraulic material handler. The machinery is simulated using Simscape, and the accuracy of the model is confirmed through experimental validation. By simulating a rational duty cycle, this study proposes two solutions for performance enhancement while maintaining the integrity of the hydraulic system. These solutions offer a balanced compromise between energy consumption and productivity and a novel control algorithm to minimize energy consumption. Most importantly, the two proposed solutions can be easily switched by the operator, which can decide to favor productivity over energy saving based on driving needs.

Keywords: non-road mobile machinery; off-highway; electrification; hydraulics; retrofitting; energy saving; load sensing

Citation: Ferrari, M.; Beltrami, D.; Uberti, S. Retrofitting Battery Electric Machinery with Unchanged Hydraulic System and Enhanced Control Strategies. *Actuators* **2024**, *13*, 191. https://doi.org/10.3390/act13050191

Academic Editors: Ioan Ursu and Matteo Davide Lorenzo Dalla Vedova

Received: 26 February 2024
Revised: 19 April 2024
Accepted: 14 May 2024
Published: 16 May 2024

1. Introduction

In recent decades, the growing focus on environmental sustainability, the reduction in greenhouse gas emissions, and the mitigation of air pollution have played a significant role in driving the adoption of electric vehicles and machinery. While consumers have become increasingly informed and cautious when choosing products, governments have concurrently been implementing stricter emission regulations [1].

The electrification of consumptions for the automotive industry is in broad daylight, but the same process has also started for the off-highway industry (also known as the Non-Road Mobile Machinery industry (NRMM)) [2]. However, some key differences exist between the two industries. First, while the architecture and size of passenger and commercial vehicles are limited in number and variety, the same does not apply to the off-highway industry [3]. Second, many small and specialized companies share an essential part of the market, which is unusual in the automotive industry.

Electrification can be seen as an enabling technology, but it also comes with new challenges and objectives. For example, although the primary objective of any machinery is to successfully execute its duty, greater emphasis has been placed on efficiency. NRMM is purchased to generate value and income; thus, this market needs to justify the higher cost of acquisition with lower costs of operation, higher productivity, and/or new purposes. Furthermore, the demand for less noisy and zero-emission machinery is expected to grow due to regulations in city centers and work environments [4]. Additionally, there is a

growing demand for such machinery in niches and work environments where managing tailpipe emissions is challenging or can adversely affect production value, like greenhouses or underground mining [5].

In general, both industry and academia are researching a variety of solutions, but defining which solution is best suited for each application is extremely challenging. This applies particularly to hydraulics, which is a key system for much of the machinery [6]. Mobile hydraulics has the highest power-to-weight ratio for actuator movement, which makes it extremely difficult to replace. At the same time, hydraulics is the biggest source of inefficiencies after the combustion engine [7], and its average energy efficiency is only as high as 21% [8]. To increase the overall efficiency of the machinery, industry and academia are researching both disruptive and incremental innovations.

The former ranges from the complete substitution of the hydraulic system with electro-mechanical actuators [9,10] to heavy modernization to various hydraulic architectures such as individual metering control [11], direct-driven hydraulics [12,13], digital hydraulics [14], and multi-chamber actuators [15].

The latter primarily depends on the use of electro-hydraulics to enhance actuation control and minimize idle losses [16]. In this regard, switching from internal combustion engines to electric machines opens great room for improvement and has the potential to facilitate energy recovery.

However, most of these efforts fail to meet the requirements of Small- and Medium-sized Enterprises (SMEs), mostly due to higher costs and the absence of economies of scale. Modeling and simulation may be a viable solution to reduce the costs partially. Indeed, big manufacturers have been developing modeling and simulation expertise for the last two or three decades, enhancing their usage of the v-cycle principles [17]. But SMEs frequently adopt the role of system integrators; they often lack extensive expertise in modeling and simulation and tend to rely on basic control methods, which can be manually adjusted by competent operators for each of the sold machinery.

In this context, this paper wants to investigate one retrofitted battery-electric machinery. The hydraulics, initially intended to work in combination with an internal combustion engine, remains unchanged in the battery-electric version, making it challenging to implement some advantageous enhancements made possible by electrification. The pump mounted on the machinery is self-regulating, so it automatically adjusts its displacement thanks to a load-sensing signal. Since the scope of the paper is to investigate the possibility of also controlling the motor speed, the pump flow will depend on two controllable variables. This approach is also followed in [18–21], in which the authors support the idea that having a control with two degrees of freedom may improve the efficiency of the system. However, all these cases are not investigated with an open hydraulic circuit with multiple actuators and are not applied to the case of Non-Road Mobile Machinery, even though Jin et al. [18] suggest this field as a possible application of their study. Indeed, in [18,19,21], different control strategies are applied to a test rig in which the actuator is replaced by a pilot pressure relief valve. Thanks to this testing methodology, it is easier to observe how this double-variable control strategy behaves at different pressure conditions. However, it does not consider the dynamic of a cylinder or a hydraulic motor. As stated by Yan et al. [20], the variation in the speed of the motor can affect the system dynamics, so it is important to consider a duty cycle applied to a physical-based model to ensure that the control does not lower the machinery's productivity. The definition of the duty cycle is not trivial. According to [22], it should be defined in collaboration with the manufacturer of the machinery since it is more aware of the actual usage. In [21], a similar control strategy is applied to a hydraulic press, which is a common application in the industrial field. However, many dissimilarities exist between this case and the common use of an NRMM. For instance, since the working cycle of an industrial machine is fixed, an accurate controlled trajectory can be defined for the industrial press. This cannot happen for an NRMM due to its several operating conditions (different loads, human-in-the-loop, etc.). In this paper, the duty cycle is defined in accordance with the manufacturer of the machinery,

and it is used to test different control strategies. It is worth noting, however, that it is not used for the definition of the control strategies.

Moreover, in all the studies shown in [18–21], the displacement is directly controllable thanks to an electric override of the load sensing system. Unfortunately, this electric override option does not exist for the hydraulic pump of this machinery. Thus, alternative control strategies are needed to avoid changing the existing hydraulic system.

Consequently, after the modeling and model validation of the machinery, this paper shows two viable solutions to improve the performance of the machinery. The former finds a good compromise between energy consumption and productivity, and the latter proposes a new control algorithm to reduce energy consumption. Because it is impossible to directly control the displacement, this second strategy aims to control the speed of the electric motor in order to force the hydraulic pump to operate at its maximum displacement value. The operator can easily switch between the two techniques since the components stay unaltered, which serves as a significant advantage.

2. Materials and Methods

2.1. The Machinery

The basis of this study is a material handler named M15 (Figure 1). The operating weight of the machinery is 14 ton, and it is manufactured by Officine Minelli s.r.l., an off-highway Small- and Medium-sized Enterprise (SME) that specializes in material handlers. The original machinery operates on ICE, while the electric variant is a retrofit of the former. Thus, the ICE and fuel tank are replaced with an electric machine and an energy storage system, respectively. In particular, a 32 kW induction motor is installed coupled with its driver, a field-oriented control (FOC) inverter designed for traction applications [23]. However, most of the components remain the same between the two versions of the machinery.

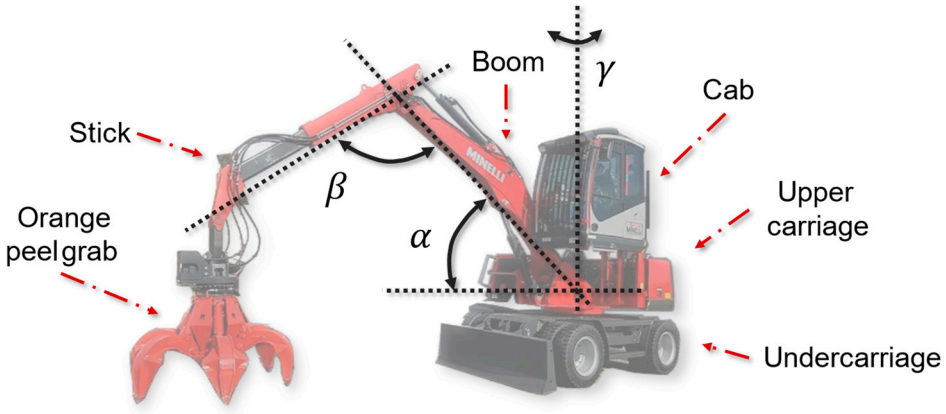

Figure 1. Substructures and most important angles (α, β, and γ) of the Minelli M15 hydraulic material handler.

As visible in Figure 1, the mechanical configuration of the M15 resembles that of an excavator, and likewise, its duty cycle. Indeed, the main duty cycle of a hydraulic material handler is based on the movements of the boom, stick, and rotation of the upper carriage. Even if the undercarriage is equipped with wheels, the impact on driving and longitudinal movements is minimal.

Being commonly employed to move scrap metal and paper waste, the orange peel grab is the most common end-effector. However, based on customer needs, alternative end-effectors, a lifting system for the cab, additional stabilizers, and an extendable second arm can be installed upon request.

In the ICE version of the machinery, the engine, the fuel tank, and the hydraulic pump are mounted in the upper carriage, and the hydraulic system is appointed to transmit power throughout the machinery. Likewise, the electric version has the energy storage system and the electric machine in place of the engine and tank situated in the upper carriage.

The hydraulic pump and the electric motor are mechanically linked by a shaft, resulting in both rotating at the same speed. A Directional Control Valve (DCV) addresses the hydraulic flow to each actuator. The movement of the spools inside the DCV is controlled by the pilot signals transmitted from the joysticks and pedals. Figure 2 illustrates a simplified scheme of the hydraulic system that powers the machinery. The pump is a self-regulating pump for open-loop operation, with a maximum flow of 150 L/min, a nominal pressure of 420 bar, and a maximum displacement of 55 cm^3/rev, which is controlled by the load-sensing signal. The DCVs that control the two arms (boom and stick) are post-compensated, while the DCV that controls the turret movement is a pre-compensated valve. This difference is necessary for safety reasons, as it prioritizes the turret movement above the two arms when flow saturation occurs. Indeed, the maximum flow of the pump is not sufficient to simultaneously drive all the actuators at their maximum speed.

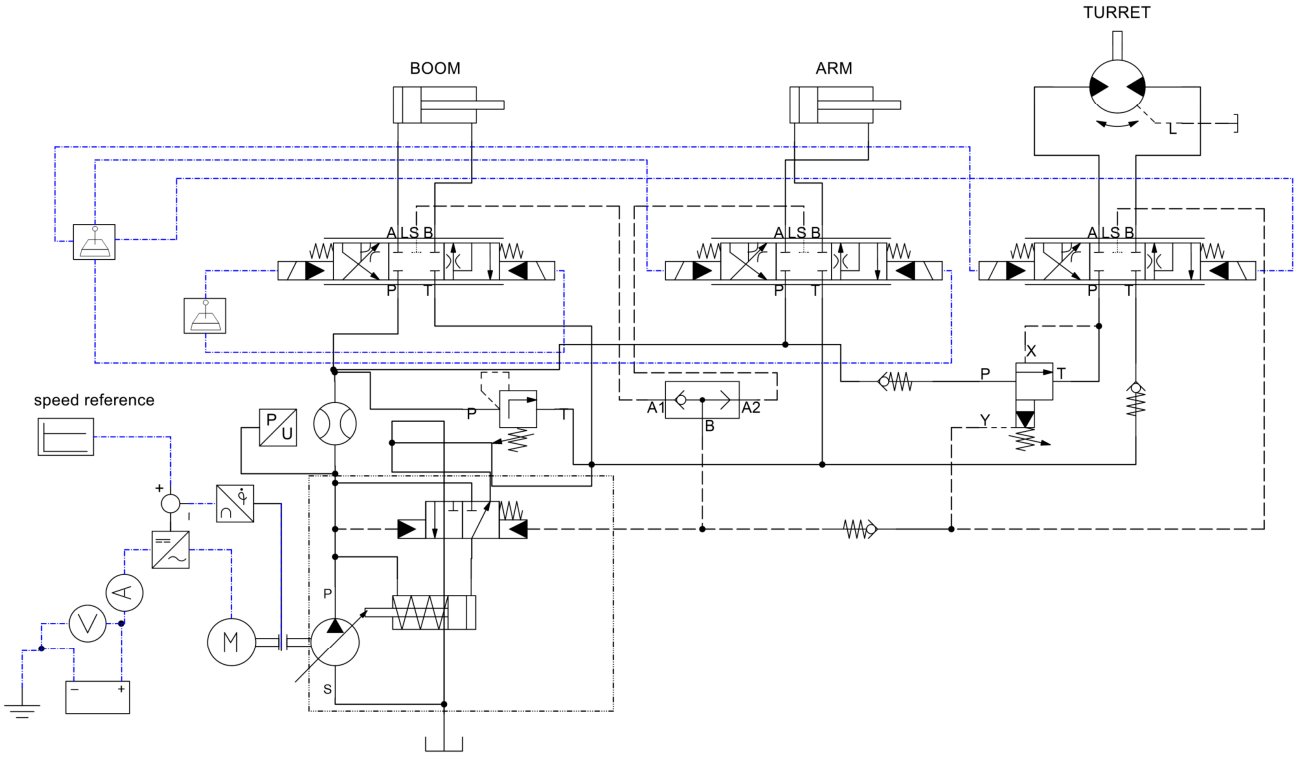

Figure 2. Simplified hydraulic scheme of the M15. Solid black lines: pressure line; black dashed lines: control line; blue dot-dash line: electrical signals.

2.2. Modeling and Simulation

Simscape and Simulink 2020b from MathWorks (Natick, MA, USA) are used to model the machinery. In particular, Simscape is designed to be an industry-oriented software that may be used by SMEs without highly qualified know-how in modeling [24,25]. As shown in Figure 3, the model is organized into subsystems.

SolidWorks is used to draw a simplified 3D model of the machinery, and the mechanical structure is imported into Simscape for the multibody simulation. However, due to the simplifications made to the CAD model, the values of inertia, mass, and all the mechanical properties deviate from their actual values. Thus, the latter are provided by the manufacturer and are manually imported into Simscape.

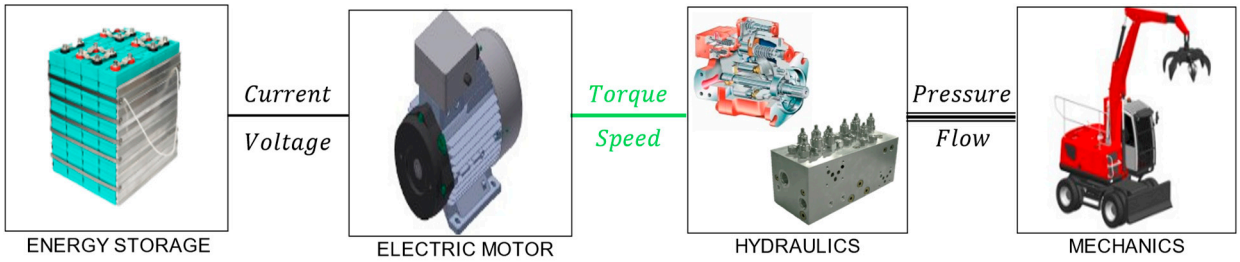

Figure 3. A simplified representation of the Simulink/Simscape model of the material handler.

Regarding the hydraulic system, some of the components are modeled by simply filling the Simscape library with the parameters given by the manufacturer. It applies to cylinders, pipe connections, and relief valves. However, for numerous other components, Simscape requires parameters that are unknown to the manufacturer, not provided by the supplier, and not published in the literature. For instance, the pre-compiled model of the directional control valve does not include post-compensator valves. So, a custom-made directional control valve is created using a combination of variable-area orifice blocks, as shown in Figure 4:

- each channel connecting a port to another (P-A, P-B, A-T, B-T) is modeled as a variable orifice;
- each variable orifice is controlled by the shifting of its spool;
- the two valves called "LS P-A" and "LS P-B" transmit the value of pressure to the load sensing circuit without any passage of oil;
- the post-compensator is modeled as a proportional 2/2 valve.

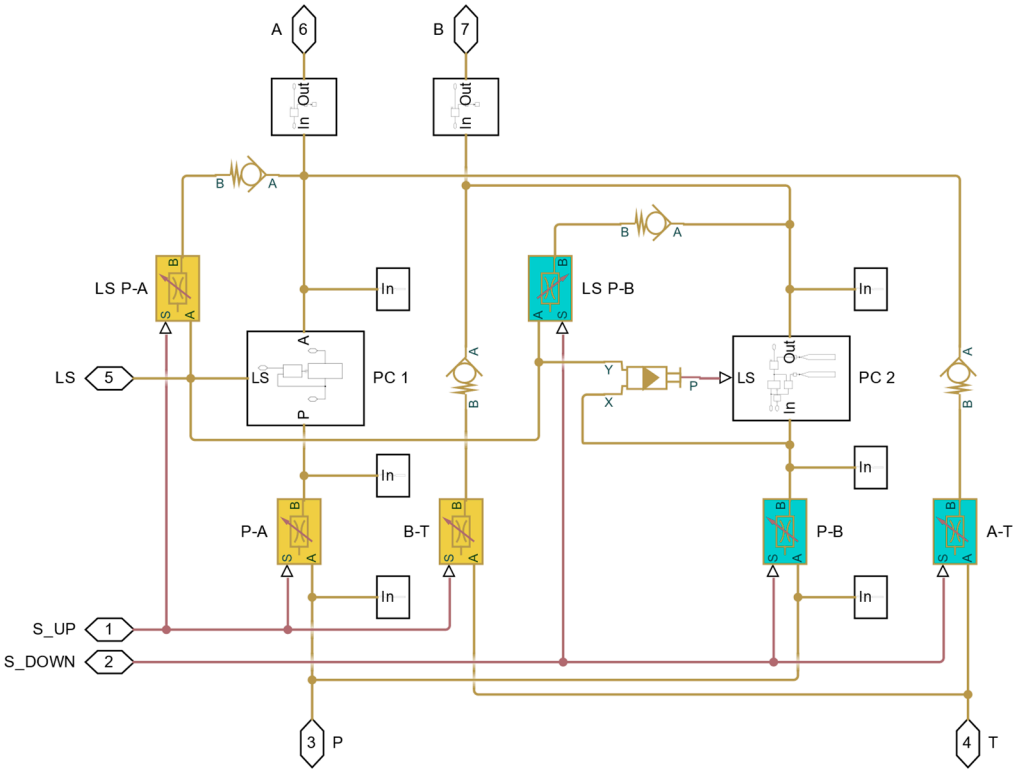

Figure 4. Simscape subsystem of the DCV. The yellow lines are the hydraulic connections. The red lines are physical signals to control the shifting of the spool.

For each valve integrated into the manifold, the supplier provided the graphs related to the spool movement, the flow through the channels PA and PB, and the pressure across the channels AT and BT (Figure 5).

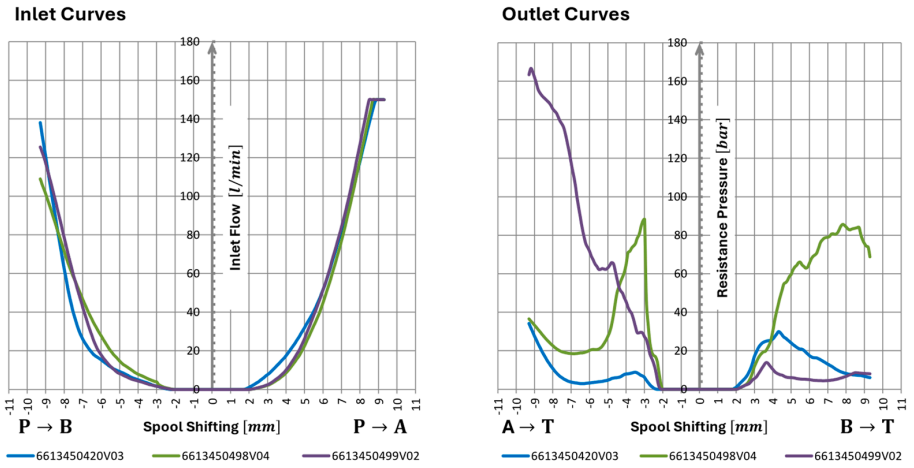

(**a**) (**b**)

Figure 5. Graph of DCVs provided by the hydraulic system supplier: characteristics flow curve between the pump port and the ports A and B (**a**); characteristics pressure curve between the tank port and the ports A and B (**b**).

The "variable displacement orifice" component requires, as inputs, the relationship between the valve's spool movement and the orifice area. This characteristic curve is not provided by the supplier; so, a Graphical User Interface (GUI) is developed to collect the supplier data and calculate a set of equivalent areas exhibiting the same behavior. The flow chart of the computation behind the GUI is visible in Figure 6, and the symbols are explained in Table 1.

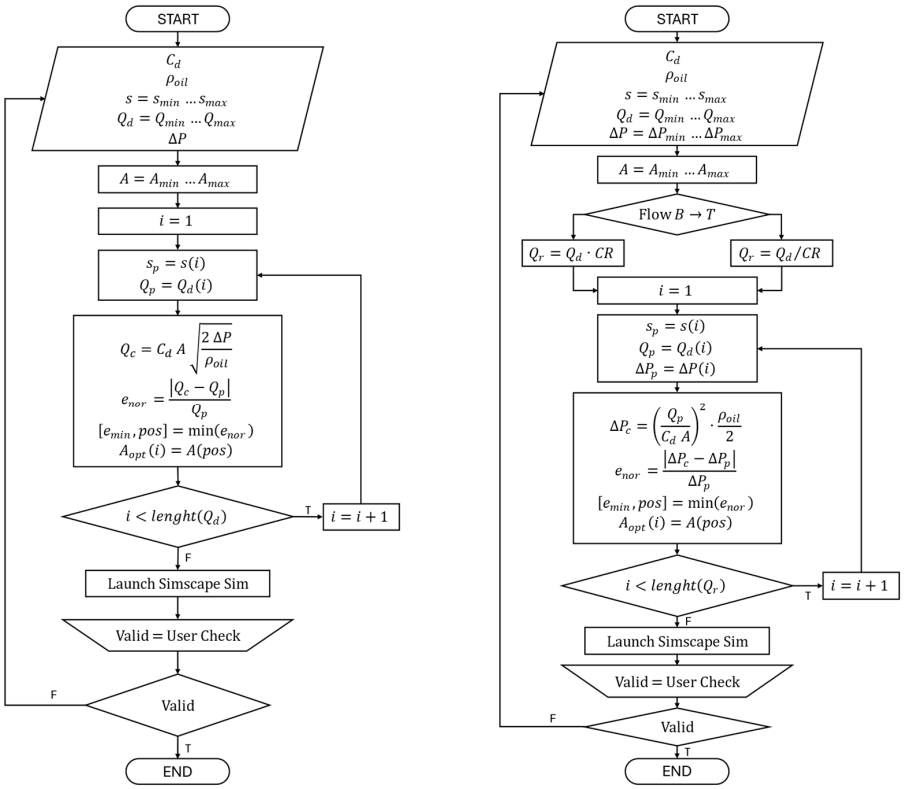

(**a**) (**b**)

Figure 6. Simplified flow chart of the GUI's computation: inlet orifices (**a**); return orifices (**b**).

Table 1. Symbols used in the flow chart of Figure 6.

Symbols	Meanings
C_d	Discharge coefficient
ρ_{oil}	Oil density
s	Spool movement
A	Orifice area
Q_d	Inlet flow from port P
Q_r	Return flow to port T
ΔP	Differential pressure across the valve
CR	Cylinder ratio

The GUI also implements a virtual test rig to evaluate the flow and pressure of the valve. The accuracy of the reverse computation performed by the GUI is verified by visually comparing the actual data with the graphs generated by the simulation, as is visible in Figure 7.

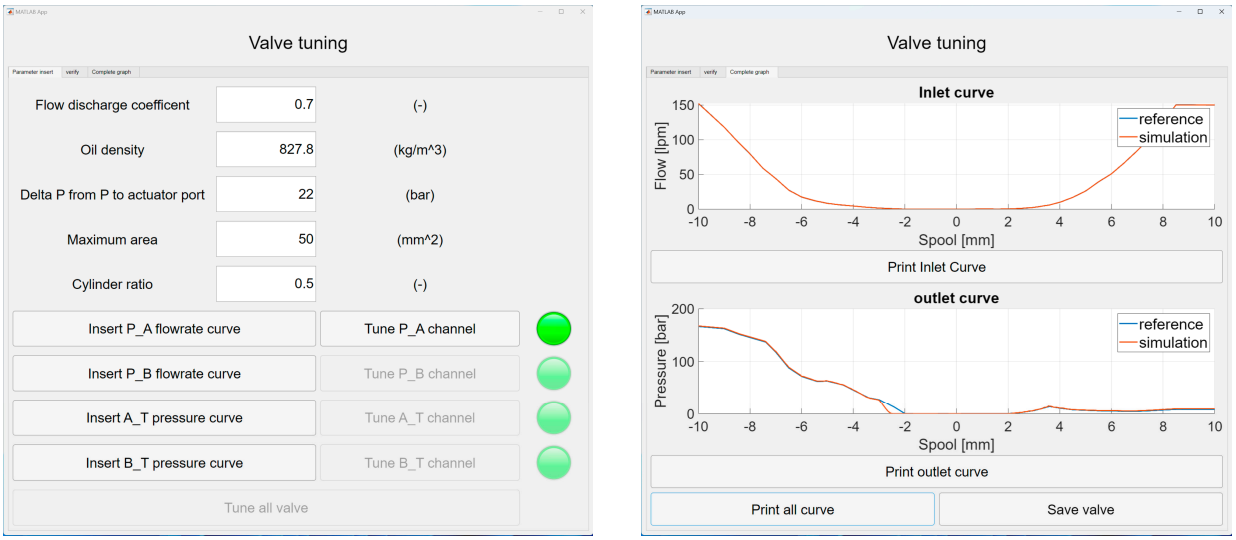

(**a**) (**b**)

Figure 7. GUI created to tune the valve model: the screen in which the user can upload the data from the supplier (**a**); visual comparison of the actual data of the supplier and the simulated ones by the GUI (**b**).

A similar process is assessed for the load-sensing circuit and load-sensing pump, whose efficiency map is automatically generated by Simscape and compared to data found in the literature for accuracy [26].

A simplified model based on a PID controller is realized to mimic the dynamic behavior of the electric motor. However, to proceed with the power consumption analysis, an efficiency map dependent on velocity and torque is created using experimental data provided by the supplier. Similarly, a 0th-order equivalent circuit model is created using official datasheets.

To validate the model, the simulation results are compared to empirical data obtained from the actual machinery. In particular, flow rate and pressure are measured at the outlet of the hydraulic pump, and the two sensors are then connected to a hydraulic-specific data logger [27], enabling the exporting of data (the position of these sensors is also visible in Figure 2). The electric motor driver facilitates the reading and storage of battery voltage, battery current, motor torque, and motor velocity using its CAN console. Lastly, the magnitude of the movements is measured by connecting the PC to the machinery's CAN

bus using a CAN-to-USB interface [28]. To ease the data post-processing, a sync signal is used to align data.

Due to the impossibility of adding pressure sensors to the actuators, the testing campaign relies on different single actuator movements:

- lowering the stick;
- rising the stick;
- lowering the boom;
- rising the boom;
- lowering the stick till the middle stroke of the cylinder;
- 90 degrees clockwise rotation of the upper carriage;
- 90 degrees counterclockwise rotation of the upper carriage to the initial position.

The results are reported in Figure 8, where the different movements are also highlighted. It is worth explaining that the very first movements of the simulation must bring the arms to the initial position of the tests. Therefore, the initial values of pressure and flow are quite different.

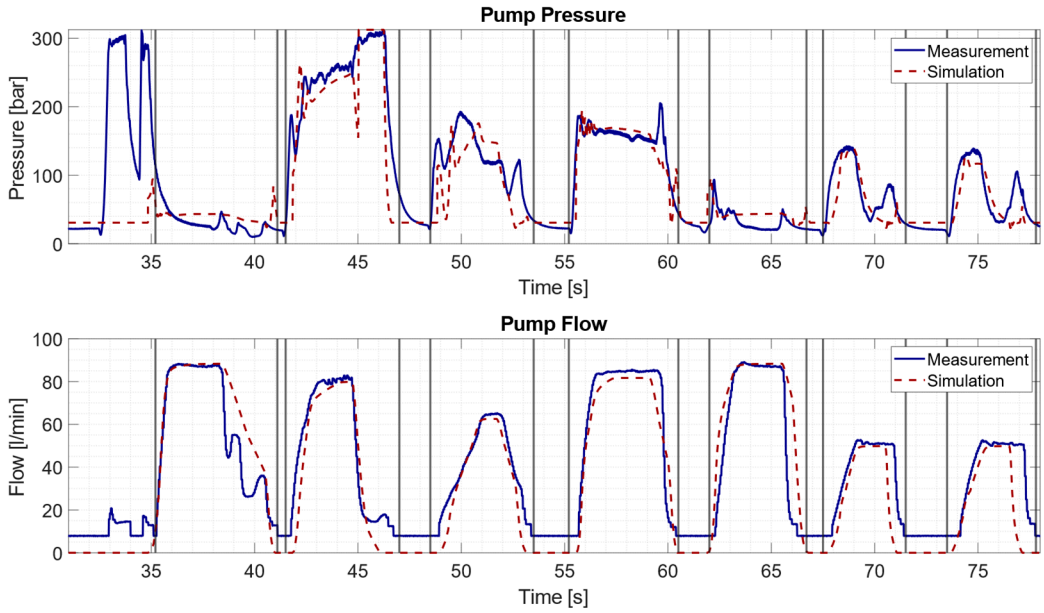

Figure 8. Comparison of pump pressure and flow rate of the actual machinery and simulated one.

The visual comparison between the actual and simulated power of the battery is shown in Figure 9.

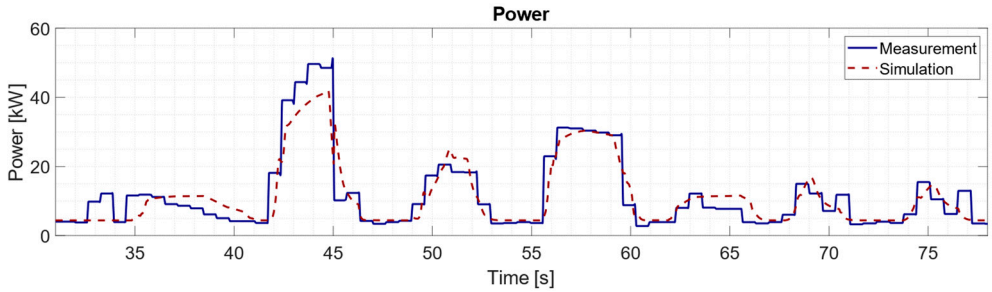

Figure 9. Comparison of the power request of the actual machinery and simulated one.

Additionally, numerical errors are also calculated to better assess the fidelity of the model (1).

$$e(t) = P_{bat_s}(t) - P_{bat_m}(t); \quad (1)$$

These values are grouped and represented by a histogram chart, which shows the probability distribution, along with the mean value (Figure 10). As demonstrated by the mean value, the model slightly overestimates the energy consumption.

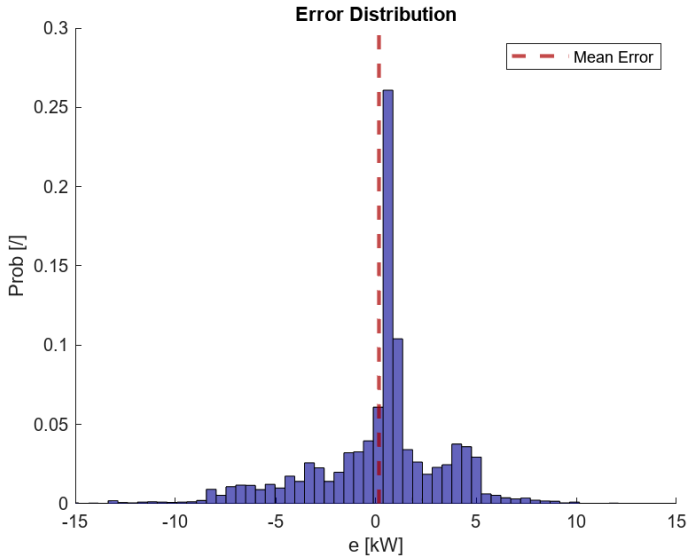

Figure 10. Error distribution of the simulation in comparison with the measured data.

However, understanding the accuracy of the model is unfeasible by using the mean value, due to the compensation between positive and negative values. Consequently, a similar approach is applied considering the errors' absolute values to create the histogram chart visible in Figure 11, whose probability distribution is exponential.

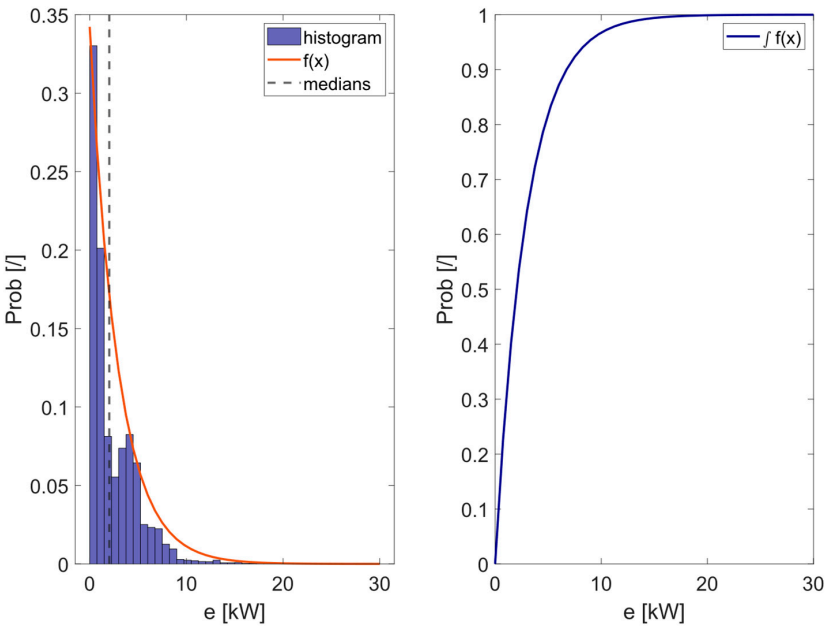

Figure 11. Statistical distribution of the absolute error.

To assess the performance of the model, other indexes are also computed, like the Integral Absolute Error (IAE) (2), its average (3), and the correlation coefficient. The IAE is useful to calculate the differences between the actual and simulated values in terms of energy. Its average, computed by dividing the IAE by the time taken to complete the movement, is useful to evaluate the error in terms of power.

$$\mathrm{IAE} = \int_0^{t_{end}} e(t)\, dt \tag{2}$$

$$\overline{\mathrm{IAE}} = \frac{\int_0^{t_{end}} e(t)\, dt}{t_{end} - 0} \tag{3}$$

Lastly, the correlation coefficient numerically assesses how alike the general trends of measurements and simulation are. All these values are visible in Table 2.

Table 2. Result of statistical evaluation.

$\bar{e}$	r	IAE	$\overline{\mathrm{IAE}}$
[kW]	**[-]**	**[kWh]**	**[kW]**
0.135	0.936	0.041	2.42

2.3. Duty Cycle

Stateflow is used to implement a duty cycle. This duty cycle is developed in collaboration with the technical office of the manufacturer. It serves as a representative example of a generic application in terms of loads, sequence of movements, and time required to return to the original position. Given the diverse range of applications in which the material handler is actually employed, establishing a singular and universally applicable duty cycle proves to be exceedingly challenging. However, the most common movement of the machinery can be identified as the act of picking and placing scrap materials, as displayed in a simplified flow chart presented in Figure 12:

- the two arms of the material handler are extended;
- the upper carriage is swung by 90 degrees;
- the end-effector grabs the load;
- the arms are raised and retracted;
- the upper carriage is swung back to the original position;
- the arms are extended;
- the load is unloaded;
- the machinery returns to the initial position.

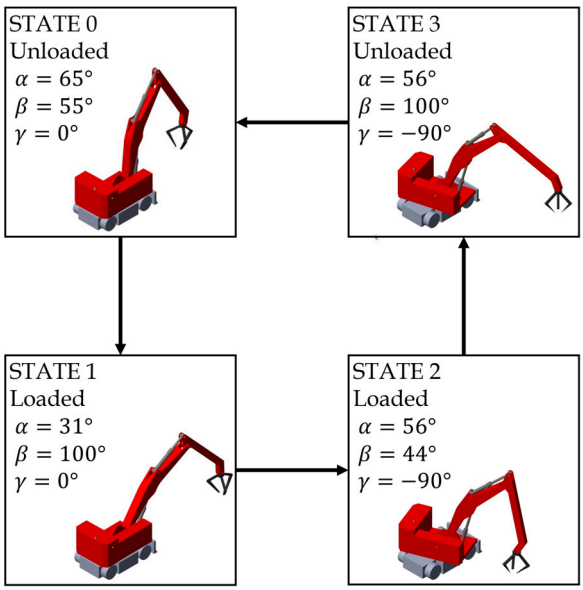

Figure 12. Flow chart of the duty cycle: alpha is the angle of the boom related to the horizontal; beta is the angle between the boom and the stick; gamma indicates the rotation of the upper carriage with respect to the undercarriage.

Several tests are performed to mimic the typical use: the operator selects a constant reference speed for the motor and performs the aforementioned duty cycle using the joysticks.

To increase the variability of the test, a MATLAB 2020b script is used to set different load values and motor speed velocity, as visible in the set of vectors of (4). This is because the machinery can handle materials with different densities, such as low-density plastic waste or high-density metallic scrap.

$$\begin{array}{c} \omega = [900\ 1200\ 1500\ 1800\ 2100\ 2400]\ \text{rpm} \\ load = [400\ 800\ 1200\ 1600]\ \text{kg} \end{array} \quad (4)$$

3. Optimization

3.1. Standard Control Strategy

First, the duty cycle is used with the standard control strategy to assess a benchmark and to evaluate how much the motor speed influences the performance of the machinery; hence, the physical-based model is used for this evaluation. The results of the combination are visible in Figures 13 and 14.

Looking at Figure 13, it is worth noting that the time duration of the duty cycle is unrelated to the load but mostly depends on the speed of the motor. This behavior is more clear at low velocity, where the curves are almost overlapping, while at high speed, there is a small difference between the tests.

Concerning the energy consumption, Figure 14 shows that it linearly increases with the load and motor speed.

The two variables exhibit opposite behavior: as the motor spins at a high velocity, the machinery consumes more energy, but the duty cycle is completed more rapidly. Both parameters are important. On the one hand, the operator needs to save enough energy to complete the working shift, but, on the other hand, productivity requires moving as much material as possible in the lowest amount of time.

Considering that, at high speed, the duration of the duty cycle reaches a plateau, while the energy consumption continues to increase, a velocity of 1600 rpm is proposed as a good compromise to be used on the machinery with the standard control strategy.

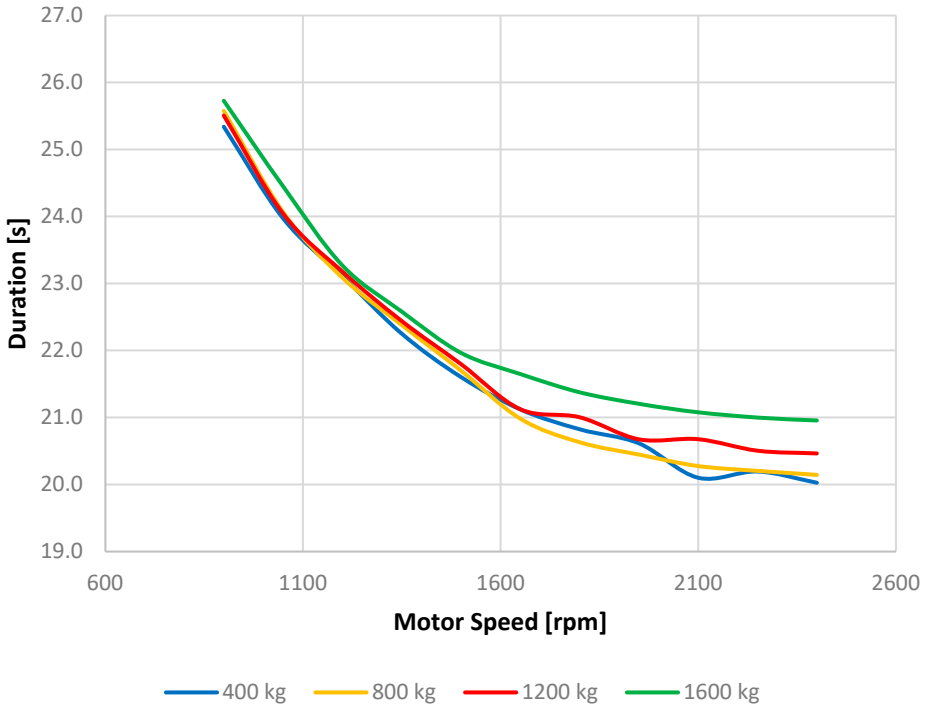

Figure 13. Duty cycle duration compared to the motor speed for the different loads.

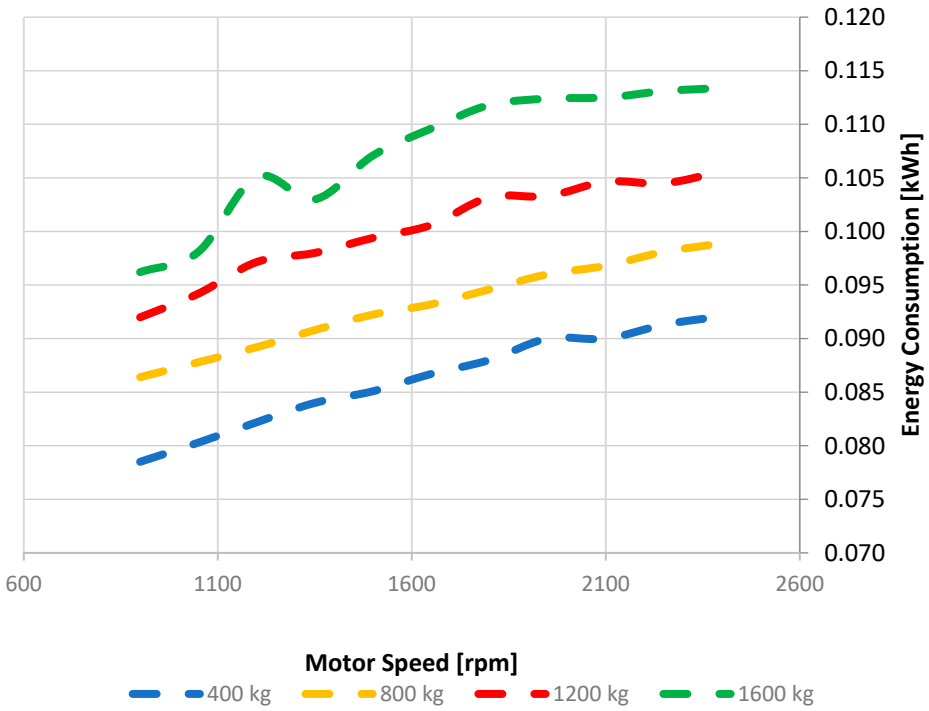

Figure 14. Duty cycle energy consumption compared to the motor speed for the different loads.

3.2. Enhanced Control Strategy

The actual machinery is equipped with a Field-Oriented Control (FOC) inverter, which is responsible for regulating the electric motor and maintaining its rotation at the intended constant velocity. This type of inverter may also be used for dynamic motor control, enabling the implementation of various control strategies.

Actually, the velocity of the motor determines the velocity of the pump, while the hydraulic system enforces the required torque. However, while internal combustion engines demand steady velocity, electric motors have higher bandwidth and are easier to control.

Therefore, it is possible to investigate new control strategies to enhance the overall efficiency of the machinery. To do so, it would be advisable to consider both the efficiency maps of the motor and the pump, which are reported in Figures 15 and 16.

In general, the efficiency of the pump is determined by three different inputs:

- the velocity of the pump. It is determined by the electric motor; thus, it may be dynamically varied by the control strategy;
- the pressure of the hydraulic system. It depends on the external loads on the actuators, along with all the pressure losses of the hydraulics;
- the requested flow. It depends on the pump's displacement, which is controlled by the load sensing control and is based on the combination of the operator requests on the joysticks and the magnitude of external loads.

The efficiency of the motor is influenced by two inputs:

- the velocity. It is related to the control applied by the inverter;
- the torque. It depends on the pressure and the displacement of the pump.

First of all, given that the electric motor has a higher efficiency compared to the pump, as also stated by Lin et al. [29], it is advisable to focus solely on the pump's efficiency while defining the control strategy.

Secondly, looking at the map in Figure 16, it is visible that the pump exhibits greater efficiency when operating at larger displacements. Since the displacement is regulated by the load sensing system, its understanding is fundamental to design an appropriate control strategy.

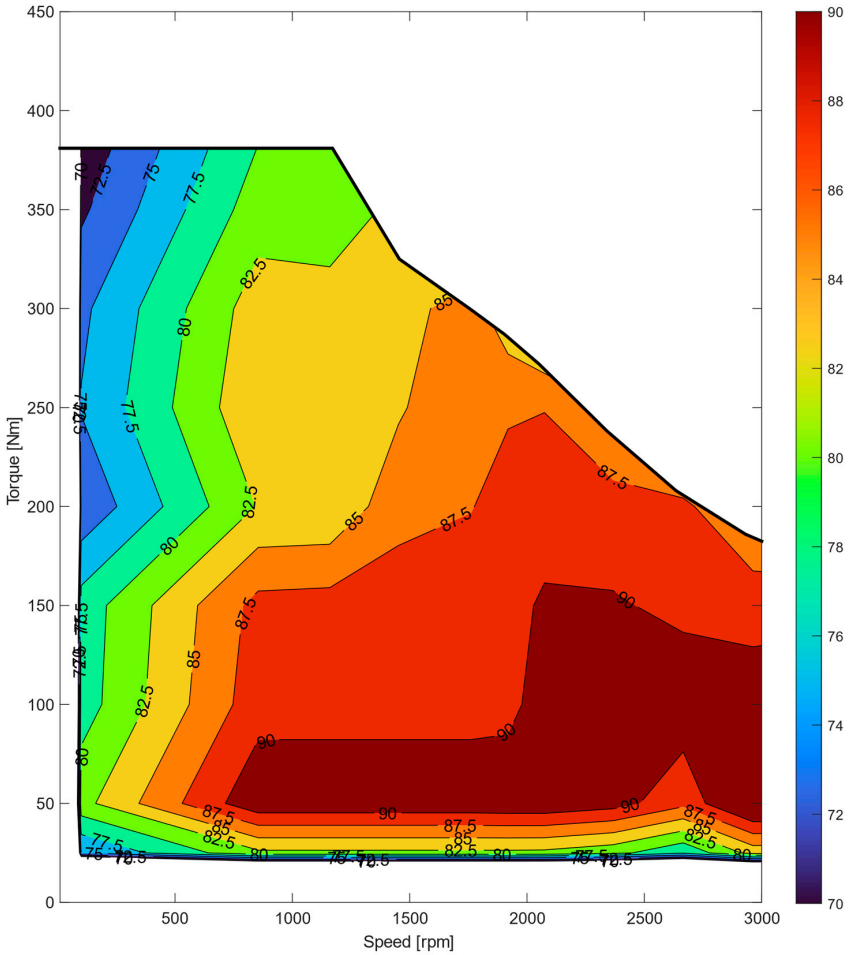

Figure 15. Efficiency map of the electric motor.

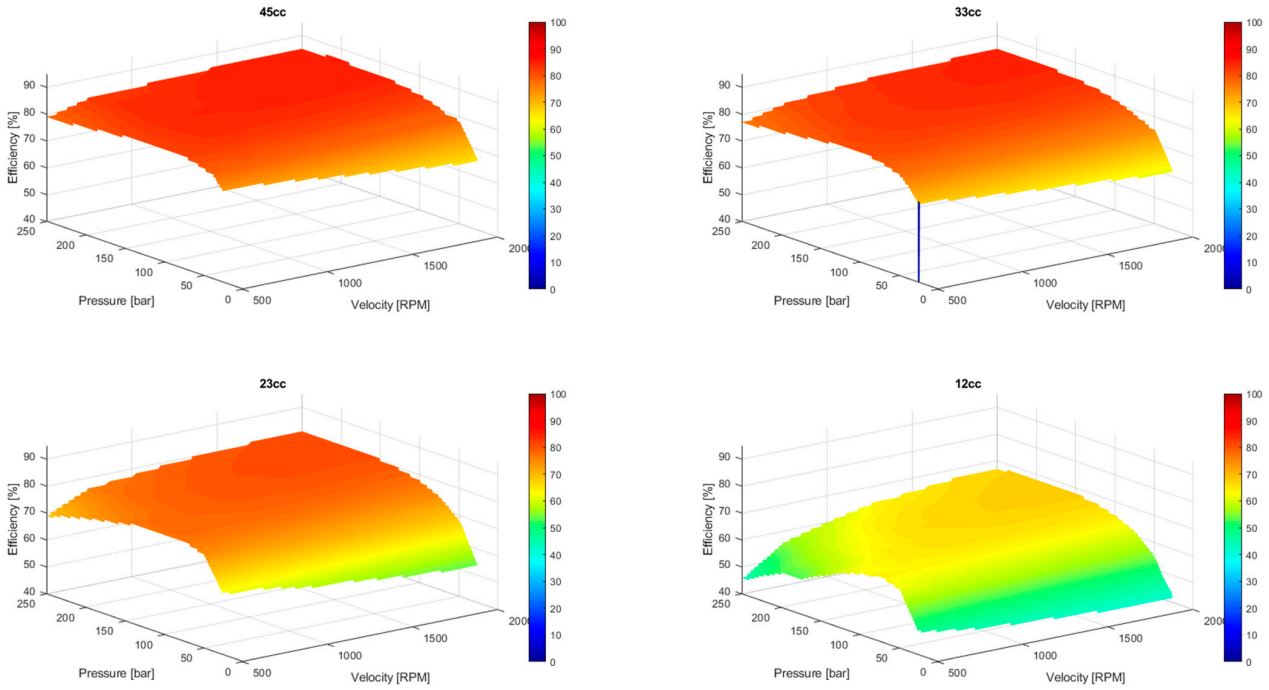

Figure 16. Efficiency map of the hydraulic pump.

By operating the actuator's joystick, a pilot pressure causes the spool of the directional control valve to move, varying its passage area. The load sensing aims to maintain a consistent pressure drop across the valve; thus, it must increase the displacement of the pump and its flow (5). From the operator's point of view, the joysticks control the velocity of the movements. Therefore, increasing the shift of the joystick results in a greater flow to the actuator.

$$Q_{\mathrm{O}} = C_{\mathrm{d}}\, A_{\mathrm{eq,\,O}} \sqrt{\frac{2\Delta p}{\rho}} \tag{5}$$

Based on these relations, it is possible to generate various look-up tables to relate the joysticks' commands and the flow needed at each side of the actuators. Finally, the speed set-point of the electric motor is calculated by dividing the desired flow by the maximum displacement (6).

$$n = Q/V_d \tag{6}$$

The proposed control strategy follows these steps, and a flow diagram of this strategy is visible in Figure 17:

- the operator moves the joysticks imposing the kinematics of the actuators;
- the joystick signals are sent to the look-up tables that calculate the flows to ensure the kinematics of each actuator;
- the total flow is computed by summing the desired flows, and moreover, it is saturated by the maximum flow accepted by the pump;
- considering the maximum displacement, the reference speed of the electric motor/hydraulic pump is computed;
- the joystick signals open the DCVs, and consequently, the pump increases the displacement to ensure the load sensing pressure drop;
- the displacement reaches its maximum value, since the minimum velocity guaranteeing the requirements is imposed.

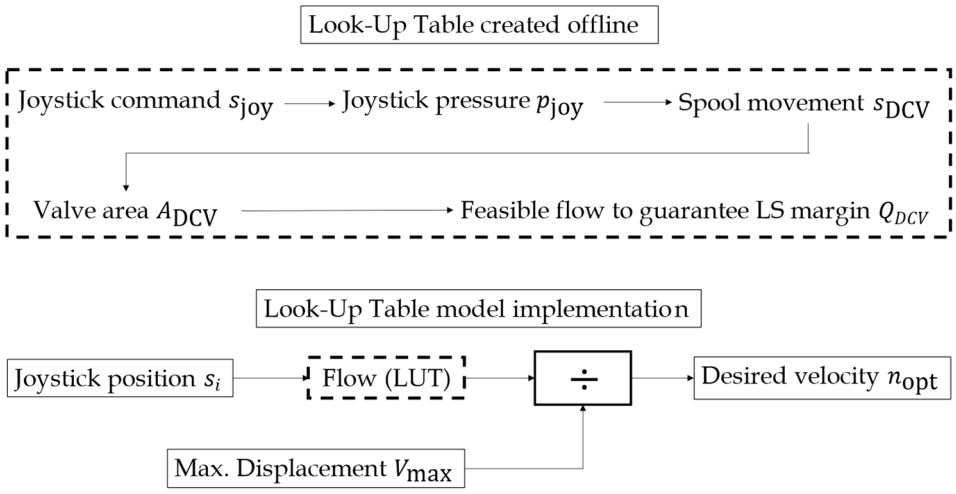

Figure 17. Flow diagram of the enhanced control strategy.

When no commands are applied to the joysticks, the electric motor is set to the idle speed of 600 rpm.

This control strategy is simulated using the synthetic duty cycle of Figure 12, and the results are visible in Figures 18 and 19.

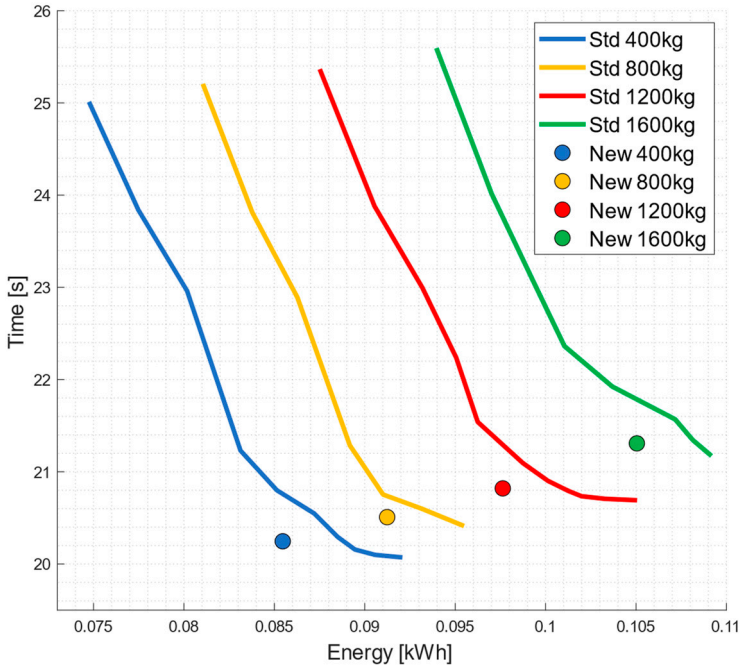

Figure 18. Results of the standard ("Std") and enhanced ("New") control strategy.

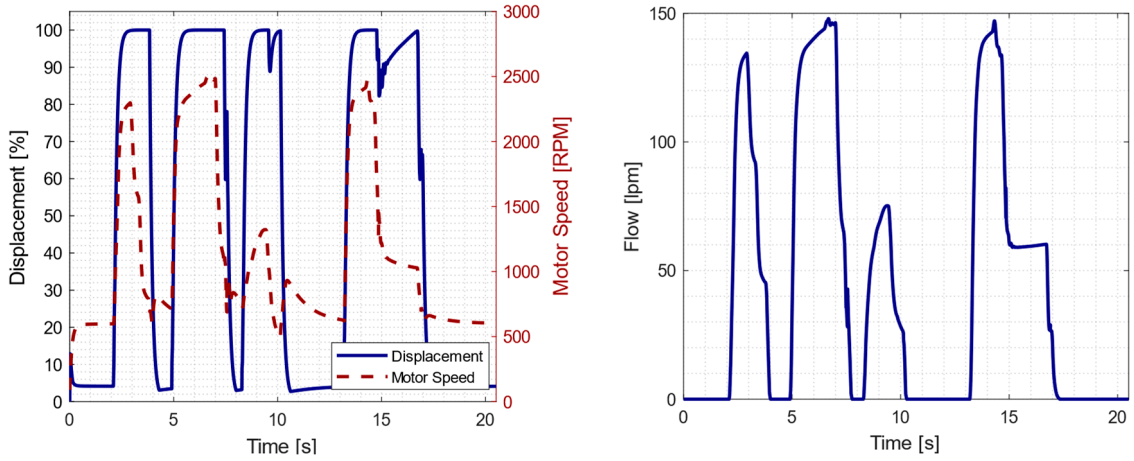

(**a**) (**b**)

Figure 19. Results of the enhanced control strategy at 800 kg: displacement and motor speed (**a**); pump flow (**b**).

4. Discussion

The graphs of Figures 18 and 19 show the energy consumption, the pump flow, the motor velocity, and the pump displacement, which is increased to its maximum value every time a command is applied. As visible in Figure 19a, by controlling the electric motor's speed, the control logic effectively forces the load sensing of the self-regulating pump to increase the displacement to its maximum value as soon as possible. The enhanced control logic allows the pump to work at a higher efficiency region, and it exploits the entire range of both displacement and speed. More importantly, this control scheme demonstrates its ability to control the load sensing system, even if it is not directly controllable.

From the energy point of view, Figure 18 highlights that this new control strategy can ensure a lower energy consumption than the previous control considering the same duty cycle time. That result can also be seen, as at the same energy consumption, this control strategy uses less time to complete the duty cycle. However, it is true that at this stage, this

control strategy focuses on the efficiency of the hydraulic pump, without considering the efficiencies of the electric drive. Consequently, this strategy is not optimal yet, and it still has room for improvement.

From the operator's point of view, this strategy neglects to allow the operator the possibility of choosing how fast the machinery works (Figure 13), thus removing the possibility of balancing the machinery between fast and precise movements. Moreover, since the control strategy has not been tested on the actual machinery, the operators' subjective feedback is still unknown.

Lastly, from the manufacturer's perspective, the hydraulic system of the machinery is completely unchanged; thus, it can be installed on both the ICE and electric variants, decreasing the supply cost. However, it is worth noting that this control logic needs testing and validation on actual machinery before it may be proposed on the market.

5. Conclusions

Emissions reduction, energy reduction, and electrification are hot research topics for off-highway machinery. In this regard, disruptive innovations, like the implementation of direct-driven hydraulics or electro-mechanical actuators, yield the most impressive results. However, the entire modification of the structure of a machinery is extremely demanding, especially for SMEs with limited production, mostly or totally based on diesel machinery. Hence, many SMEs are designing retrofitting variants of standard diesel engine machinery, where the electric motor simply replaces the combustion engine and is used at constant speed. However, different control strategies may bring better results by taking advantage of the ease of control of the electric motors. This paper investigates this possibility by modeling and simulating a retrofitted electric material handler. First, to create a benchmark on a common duty cycle, this study simulates the constant speed control strategy implemented on the actual machinery, also proposing a reference speed to balance the duty cycle's duration and energy consumption. Then, the basis of a new control strategy is explained and implemented in the model. The control strategy optimizes pump efficiency by assessing the flow request at the cabin joysticks and adjusting the electric motor rotational velocity, knowing that the pump efficiency increases at higher displacements. The simulated results show that this strategy improves energy consumption with unchanged hydraulics. Furthermore, by keeping the hydraulics unchanged, the operator can select the best control strategy based on current needs, expanding the flexibility of the machinery. Similarly, following the same approach, it may be possible to investigate other solutions for energy consumption optimization. Even if more disruptive solutions may bring better results, this intermediate solution is also easier to adopt for SMEs on their electric retrofitted portfolio and may bring immediate results.

Author Contributions: Conceptualization, M.F., D.B. and S.U.; methodology, M.F. and D.B.; software, M.F. and D.B.; validation, M.F. and D.B.; formal analysis, M.F.; investigation, M.F. and D.B.; writing—original draft preparation, M.F. and D.B.; writing—review and editing, S.U.; visualization, D.B.; supervision, S.U.; project administration, S.U.; funding acquisition, S.U. All authors have read and agreed to the published version of the manuscript.

Funding: This research was funded by the Italian Government fund PON DM1061 of "Ministero dell'Università e della Ricerca".

Data Availability Statement: Data presented in this study are available upon request to the corresponding author. The data are not publicly available due to the privacy policy of the University of Brescia.

Acknowledgments: The authors sincerely thank Officine Minelli s.r.l. in the person of Graziano Bodei, Marcello Galperti and Roberto Fiorini for their ongoing assistance.

Conflicts of Interest: The authors declare no conflicts of interest.

References

1. Dallman, T.; Menon, A. *Technology Pathways for Diesel Engines Used in Non-Road Vehicles and Equipment*; International Council on Clean Transportation (ICCT): Washington, DC, USA, 2016.
2. Beltrami, D.; Iora, P.; Tribioli, L.; Uberti, S. Electrification of Compact Off-Highway Vehicles—Overview of the Current State of the Art and Trends. *Energies* **2021**, *14*, 5565. [CrossRef]
3. Malavatu, J.; Kandke, S.R.; Gupta, S.; Agrawal, B. Design Challenges in Electrification of Off-highway Applications. In Proceedings of the 2019 IEEE Transportation Electrification Conference, ITEC-India 2019, Bengaluru, India, 17–19 December 2019. [CrossRef]
4. Public Buyers Community. Joint Statement of Demand of Zero Emission Construction Sites Working. Available online: https://public-buyers-community.ec.europa.eu/resources/joint-statement-demand-zero-emission-construction-sites-working-group (accessed on 22 August 2023).
5. Lajunen, A.; Sainio, P.; Laurila, L.; Pippuri-Mäkeläinen, J.; Tammi, K. Overview of Powertrain Electrification and Future Scenarios for Non-Road Mobile Machinery. *Energies* **2018**, *11*, 1184. [CrossRef]
6. Fassbender, D. Towards Energy-Efficient Electrified Mobile Hydraulics Considering Varying Application Conditions. Ph.D. Thesis, Tampere University, Tampere, Finland, 2023.
7. An, K.; Kang, H.; An, Y.; Park, J.; Lee, J. Methodology of Excavator System Energy Flow-Down. *Energies* **2020**, *13*, 951. [CrossRef]
8. Love, L.J. *Estimating the Impact (Energy, Emissions and Economics) of the US Fluid Power Industry*; Oak Ridge National Laboratory: Oak Ridge, TN, USA, 2012. [CrossRef]
9. Bobcat. T7X All Electric Compact Track Loader—Bobcat Company. Bobcat. Available online: https://www.bobcat.com/na/en/equipment/future-products/t7x-electric-compact-track-loader (accessed on 7 October 2022).
10. Wang, L.; Zhao, D.; Li, Y.; Du, M.; Chen, H. Energy management strategy development of a forklift with electric lifting device. *Energy* **2017**, *128*, 435–446. [CrossRef]
11. Mahato, A.C.; Ghoshal, S.K. Energy-saving strategies on power hydraulic system: An overview. *Proc. Inst. Mech. Eng. Part I J. Syst. Control. Eng.* **2021**, *235*, 147–169. [CrossRef]
12. Zhang, S.; Minav, T.; Pietola, M. Decentralized Hydraulics for Micro Excavator. In Proceedings of the 15th Scandinavian International Conference on Fluid Power, 15th Scandinavian International Conference on Fluid Power, Fluid Power in the Digital Age, SICFP'17, Linköping, Sweden, 7–9 June 2017; pp. 187–195. [CrossRef]
13. Zhang, S.; Minav, T.; Pietola, M.; Kauranne, H.; Kajaste, J. The effects of control methods on energy efficiency and position tracking of an electro-hydraulic excavator equipped with zonal hydraulics. *Autom. Constr.* **2019**, *100*, 129–144. [CrossRef]
14. Pellegri, M.; Green, M.; Macpherson, J.; McKay, C.; Caldwell, N. Applying a multi-service digital displacement® pump to an excavator to reduce valve losses. In Proceedings of the 12th International Fluid Power Conference (12. IFK), Dresden, Germany, 12–14 October 2020; Technische Universität Dresden: Dresden, Germany, 2020; Volume 2, pp. 59–68. [CrossRef]
15. Habibi, S.; Goldenberg, A. Design of a new high performance electrohydraulic actuator. In Proceedings of the 1999 IEEE/ASME International Conference on Advanced Intelligent Mechatronics (Cat. No.99TH8399), Atlanta, GA, USA, 19–23 September 1999; pp. 227–232. [CrossRef]
16. Fassbender, D.; Zakharov, V.; Minav, T. Utilization of electric prime movers in hydraulic heavy-duty-mobile-machine implement systems. *Autom. Constr.* **2021**, *132*, 103964. [CrossRef]
17. Cosadia, I.; Silvestri, J.J.; Papadimitriou, I.; Maroteaux, D.; Obernesser, P. *Traversing the V-Cycle with a Single Simulation—Application to the Renault 1.5 dCi Passenger Car Diesel Engine*; SAE International: Warrendale, PA, USA, 2013. [CrossRef]
18. Jin, R.; Huang, H.; Li, L.; Zhu, L.; Liu, Z. Energy Saving Strategy of the Variable-Speed Variable-Displacement Pump Unit Based on Neural Network. *Procedia CIRP* **2019**, *80*, 84–88. [CrossRef]
19. Reichert, W.; Leonhard, A.; Päßler, T.; Kurth, R.; Ihlenfeldt, S. Implementation of an Electro-Hydraulic Drive Unit with Two Control Variables in a Drawing Cushion Application. *Eng. Proc.* **2022**, *26*, 18. [CrossRef]
20. Yan, Z.; Ge, L.; Quan, L. Energy-Efficient Electro-Hydraulic Power Source Driven by Variable-Speed Motor. *Energies* **2022**, *15*, 4804. [CrossRef]
21. Huang, H.; Jin, R.; Li, L.; Liu, Z. Improving the Energy Efficiency of a Hydraulic Press Via Variable-Speed Variable-Displacement Pump Unit. *J. Dyn. Syst. Meas. Control* **2018**, *140*, 111006. [CrossRef]
22. Bertini, A.; Ceraolo, M.; Lutzemberger, G. Development of a hybrid skid loader through modelling. In Proceedings of the 2012 IEEE International Energy Conference and Exhibition (ENERGYCON), Florence, Italy, 9–12 September 2012; pp. 1022–1027. [CrossRef]
23. Zapi S.p.A. *Datasheet—ZAPI AC3*; Zapi S.p.A. 2015. Available online: www.zapispa.it (accessed on 1 June 2022).
24. The MathWorks Inc. Simscape—MATLAB. Available online: https://www.mathworks.com/products/simscape.html (accessed on 1 December 2021).
25. Beltrami, D.; Ferrari, M.; Iora, P.G.; Uberti, S. *Application of Physics-Based Modeling Techniques as a Tool to Help the Development of More Electrified Off-Highway Machinery*; Springer: Cham, Switzerland, 2024; pp. 497–504. [CrossRef]
26. Kauranne, H. Effect of Operating Parameters on Efficiency of Swash-Plate Type Axial Piston Pump. *Energies* **2022**, *15*, 4030. [CrossRef]
27. Hydrotechnik GmbH. *MultiHandy 3050*; Hydrotechnik GmbH: Limburg an der Lahn, Germany, 2024.

28. PEAK System. *Datasheet—PEAK PCAN-USB*; PEAK System. 2021. Available online: https://www.peak-system.com/PCAN-USB.199.0.html?&L=1 (accessed on 23 October 2023).
29. Lin, T.; Lin, Y.; Ren, H.; Chen, H.; Li, Z.; Chen, Q. A double variable control load sensing system for electric hydraulic excavator. *Energy* **2021**, *223*, 119999. [CrossRef]